Folia Microbiologica
https://doi.org/10.1007/s12223-026-01489-z

RESEARCH

Design, synthesis, and antimicrobial evaluation of heteroaromatic or acyl-substituted benzenesulfonamide-linked aminoquinolinequinones

Hatice Yıldırım[1] · Mahmut Yıldız[2] · Nilüfer Bayrak[3] · Bekir Özer[4] · Emel Mataracı-Kara[4] · Mayram Hacıoğlu[4] · Abanish Biswas[5] · Berna Özbek-Çelik[4] · Venkatesan Jayaprakash[5] · Amaç Fatih TuYuN[3]

Received: 29 January 2026 / Accepted: 17 April 2026
© The Author(s) 2026

Abstract

A series of aminated quinolonequinones (**AQQ1-13**) was synthesized from quinolinequinone and substituted aromatic amines containing a sulfonamide group with conformationally restricted heterocyclic structures or an acyl group. The obtained AQQs were characterized by various spectroscopic techniques including FTIR, NMR, and MS analyses. Structural modifications of the sulfonamide group in these compounds were selected by introducing various heterocyclic substituents, such as isoxazole, thiadiazole, pyridine, pyrimidine, pyrazine, and pyridazine, or by attaching acyl groups (acetyl or benzamide) with different substituents. Some of the synthesized AQQs exhibited antifungal activity against the tested strains, with potencies comparable to the reference drugs under the tested conditions. Noticeably, **AQQ5** with thiadiazole moiety attached to the sulfonamide group showed inhibitory activity against *C. albicans* (MIC: 19.53 µg/mL). The most active compound **AQQ5** also showed the best antifungal potency towards to other two fungi (*C. parapsilosis* and *C. tropicalis*). However, it should be noted that antifungal activity was evaluated only against ATCC strains. Considering the increasing prevalence of antifungal resistance, these results may not fully reflect the efficacy against clinical isolates. Antifungal resistance may render the antifungal activity already seen against ATCC strains ineffective in clinical isolates. Yet the putative target, farnesyl pyrophosphate synthase identified through in silico protocols suggests that farnesyl pyrophosphate synthase may be a potential target, warranting further experimental validation.

Keywords Antimicrobial activity · Sulfonamides · Bactericidal effect · Quinolinequinone

Introduction

In the human body, there are microorganisms called normal flora that do not cause disease unless the immune system is weakened or they enter a sterile part of the body, as well as microorganisms called pathogens that cause disease when they enter the body, such as viruses, bacteria, fungi, and parasites (Alberts et al. 2002). Pathogens need a host to survive and can enter their hosts through areas such as the skin, urogenital, gastrointestinal, and respiratory tracts (Prasad, 2007). Once in a host's body, they can escape the body's immune response and multiply (Mak and Saunders 2007). The ability of an infectious agent to cause disease in a susceptible host is called pathogenicity, and the degree of disease it causes is called virulence (Shapiro-Ilan et al. 2005). The virulence of a pathogenic microorganism is associated with the genetic, biochemical, and structural factors that

✉ Amaç Fatih TuYuN
aftuyun@gmail.com; aftuyun@istanbul.edu.tr

1 Department of Chemistry, Faculty of Engineering, Istanbul University - Cerrahpasa, Avcılar, Istanbul, Turkey

2 Department of Chemistry, Faculty of Science, Gebze Technical University, Gebze, Kocaeli 41400, Turkey

3 Department of Chemistry, Faculty of Science, Istanbul University, Fatih, Istanbul 34134, Turkey

4 Department of Pharmaceutical Microbiology, Pharmacy Faculty, Istanbul University, Beyazit, Istanbul 34116, Turkey

5 Department of Pharmaceutical Sciences and Technology, Birla Institute of Technology, Ranchi, Jharkhand 835215, India

Published online: 25 April 2026

cause disease (Jedrzejas 2001). Nobel Prize-winning scientist Koch's experiments on laboratory animals to design a systematic approach to confirm causal relationships between diseases and specific pathogens, and subsequent advances in microbiology, were critical steps that revolutionized the development of infection science (Cochran et al. 2000).

Bacterial and fungal infections pose a great risk to humanity due to their ability to spread to host tissues in individuals with weakened immune systems and the emergence of resistant strains. Fungal species such as *Candida*, *Aspergillus*, and *Cryptococcus* in particular have been reported to cause infections with high mortality rates (Martins-Santana et al. 2023). In 2021, 4.71 million deaths were associated with bacterial antimicrobial resistance (AMR), and among these deaths, methicillin-resistant *Staphylococcus aureus* showed the highest increase worldwide, and resistance to carbapenems among Gram-negative bacteria increased more than all other antibiotic classes. It is stated that an estimated 8.22 million AMR-related deaths could occur in 2050 and that the development of a Gram-negative drug pipeline is essential to prevent AMR deaths (Naghavi et al. 2024). Even more alarming are the pessimistic scenarios of global infection by pathogenic microorganisms, with multidrug-resistant (MDR) microorganisms becoming increasingly more prevalent than drug-sensitive strains, and MDR microorganisms beginning to have an intercontinental impact (Pitout and Laupland 2008; Alexander et al. 2013; Arendrup 2014).

One of the most important and exciting areas of study at the intersection of synthetic chemistry and medicinal chemistry is the development of new agents that are broad-spectrum and effective against drug resistance. In the arena where pathogenic microorganisms, which are the cause of infectious diseases that threaten humanity in recent years, are combated, it has been observed that microorganisms have gained an advantage over humanity thanks to their extraordinary spreading speed and the resistance they have developed against compounds that currently have drug status. In this regard, scientists continue their work without interruption on the design, synthesis, and in vitro and in vivo (animal model) testing of promising chemical molecules for the preparation of new and more effective antipathogenic agents that have high potency and selectivity as well as low toxicity and reduce or prevent side effects.

The 1,4-quinone moiety is widely recognised as a fundamental core structure in medicinal chemistry and drug development (Wellington 2015; de Carvalho et al. 2021; Devi et al. 2022; Mone et al. 2023). It is a key core structure of many naturally occurring compounds that are biologically active as well as preclinical or clinical therapeutic agents shown in Fig. 1. Medicinal chemists and scientists from around the world have taken a keen interest in 1,4-quinones due to their multifunctional and redox-active core properties (Kuang et al. 2018; Dahlem Junior et al. 2022; Chan-Zapata et al. 2023; Navarro-Tovar et al. 2023). Numerous types of active heterocyclic 1,4-quinones have been made through ongoing structural modifications, resulting in them being useful building blocks for the development of novel lead structures. So far, many different types of heterocyclic 1,4-quinones, including pyrimidine (Kuang et al. 2018), pyridine (Alfadhli et al. 2016; Ibacache et al. 2016, 2018; Valderrama et al. 2016; Egu et al. 2017; Defant and Mancini 2019; Santoso et al. 2019; Kruschel et al. 2020, 2024), pyrazine (Keinan et al. 2008), pyridazine (Shen et al. 2010), furan (Hu et al. 2005), and thiophene (Valderrama et al. 1999), have been extensively explored and used in drug research and development. The benzenesulfonamide analogues are used as nucleophilic reagents in the development of therapeutic agents because of their substantial and well-established pharmacological potential (Elgemeie et al. 2019; Elsayad et al. 2024). As a continuation of our long-term efforts to identify promising therapeutic lead structures with antimicrobial and/or anticancer effects, herein, we report the synthesis, characterisation, and evaluation of antimicrobial properties of a series of benzenesulfonamide-containing heterocyclic 1,4-quinones. Their antifungal and antibacterial action was studied in vitro, and the action mechanism of benzenesulfonamide-containing heterocyclic 1,4-quinones was suggested using molecular docking.

Results and discussion

Chemistry

We previously reported a series of aminated quinolinequinones (AQQs) incorporating aromatic amine moiety substituted with versatile groups, including strong electron-donating groups (EDGs), moderate EDGs, and electron-withdrawing groups (EWGs) at different positions on the phenyl ring as selective antimicrobial agents. The developed aminated QQs showed significant in vitro inhibitory activity against gram-positive bacteria and also fungi (Mataraci-Kara et al. 2022a, b, c; Yildirim et al. 2022a, b). Analysing these results, we identified both the quinolinequinone core and the aromatic amine moiety as the elements of great in vitro inhibitory activity and designed a new series utilising this chemical moiety as a template. In our ongoing efforts to identify new selective antibacterial and/or antifungal lead structures, we explored isosteric replacement strategies. Specifically, various groups attached to the aromatic amine moiety were replaced with a sulfonamide group, followed by the introduction of either conformationally restricted heterocyclic structures or an acyl group onto the sulfonamide moiety, as illustrated in Fig. 2. Structural modification of the sulfonamide group of these compounds by either the introduction of different heterocyclic substituent, including isoxazole,

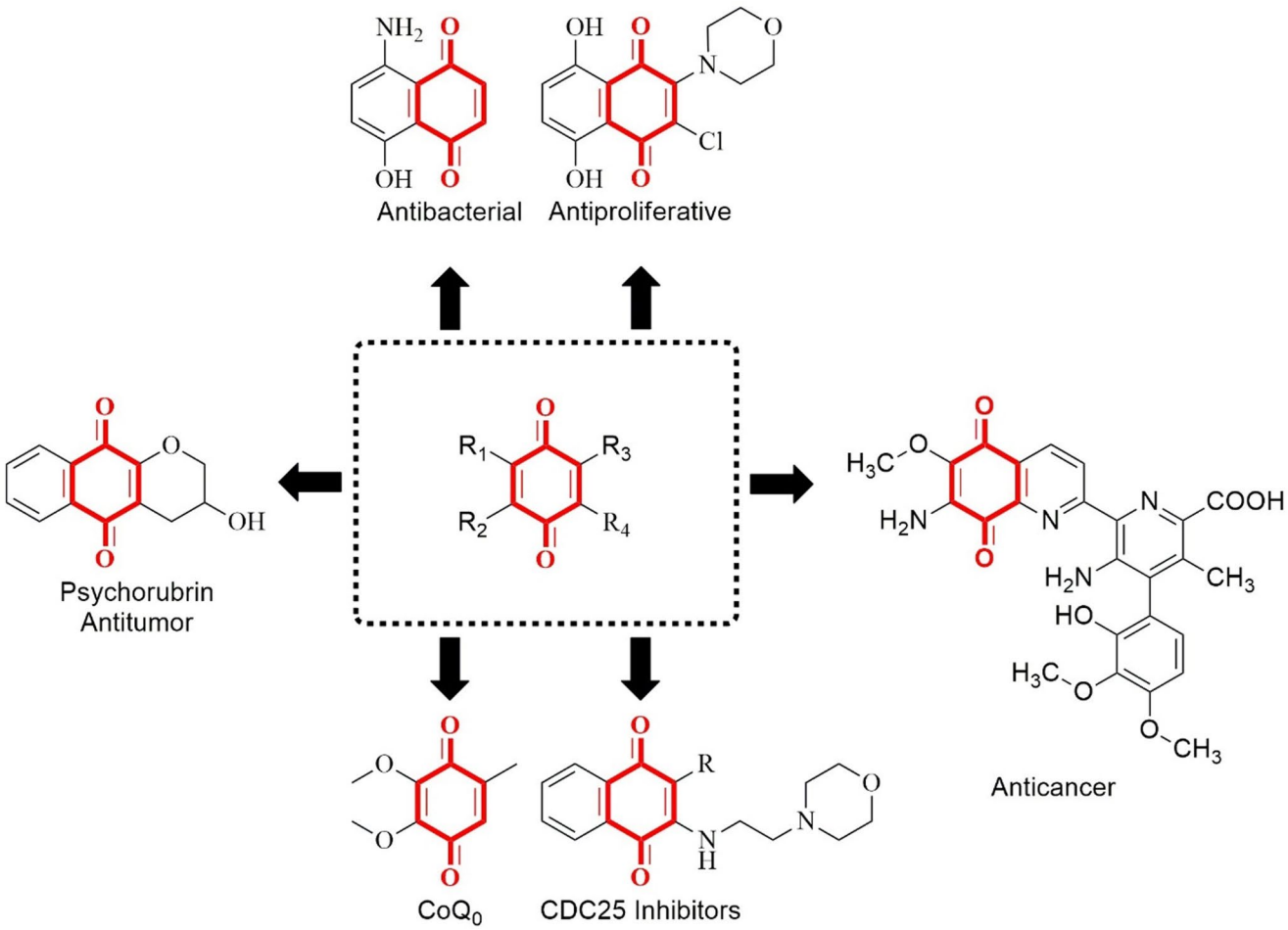


Fig. 1 Structurally diverse biologically active compounds containing 1,4-quinone moiety

thiadiazole, pyridine, pyrimidine, pyrazine, and pyridazine or acyl group (acetyl and benzamide) with different substituent(s), was conducted. Previous studies have suggested that the incorporation of EDGs, such as methoxy or methyl substituent(s) within the sulfonamide moiety, has been associated with increased potency (Sharma et al. 2023; Chen et al. 2024).

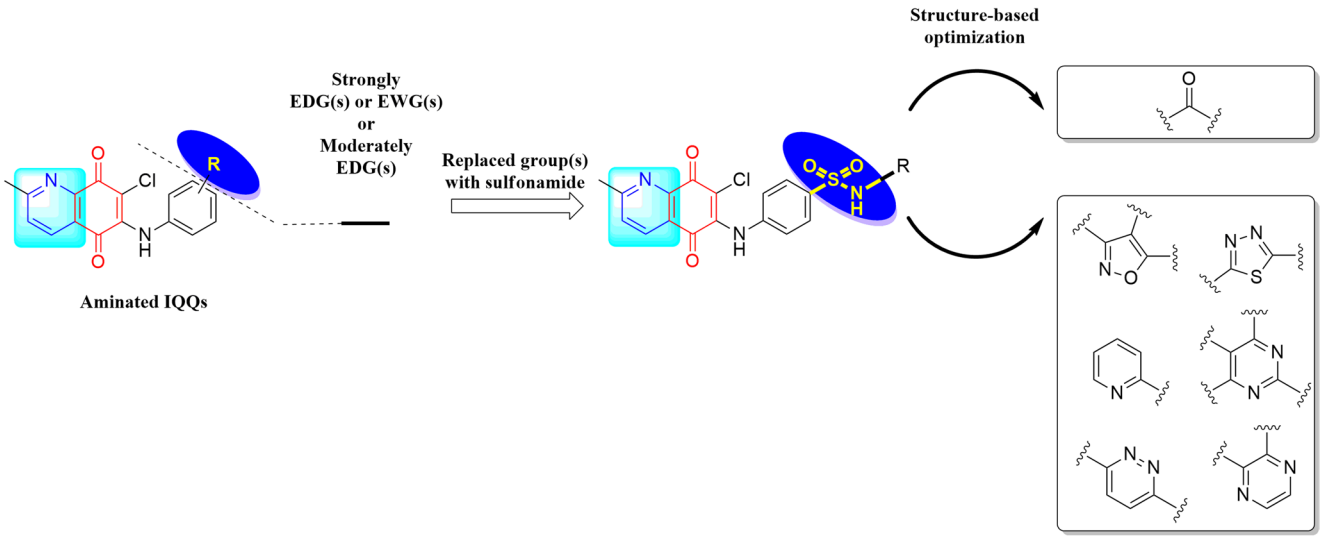
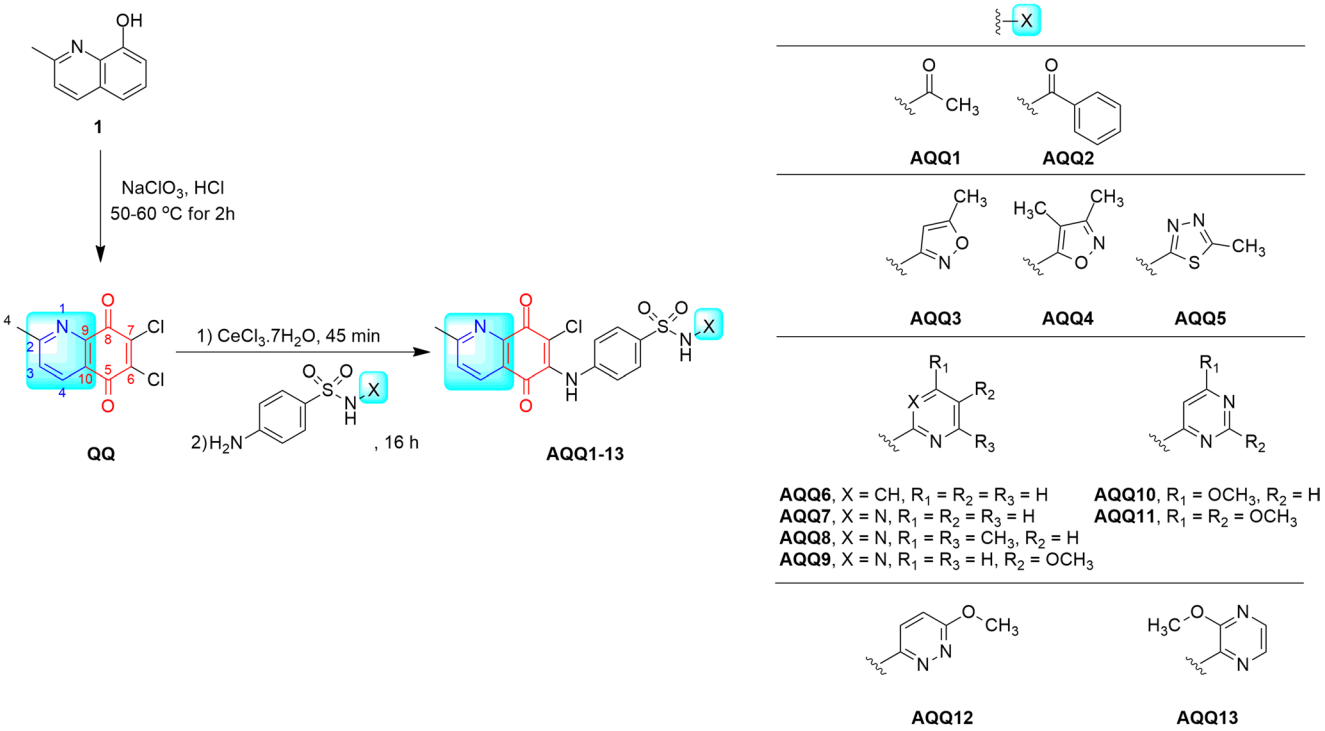


Fig. 2 Optimisation of aminated QQs with sulfonamide replacement

Despite extensive literature on the use of benzenesulfonamides as valuable reagents in synthesis (Elgemeie et al. 2019), we have found only a few examples on the synthesis of (hetero)cyclic quinones using benzenesulfonamides (Yanni et al. 1991; Lawrence et al. 2010; Pingaew et al. 2015; Uysal et al. 2021). In this effort, starting from commercially available 8-hydroxyquinoline (**1**), the target compounds (aminated quinolinequinones, **AQQ1-13**) as outlined in Scheme 1 were synthesised *via* a concise and well-established synthetic route (Shaikh et al. 1986). Treating **1** with sodium chlorate ($NaClO_3$) in concentrated HCl solution gave chlorinated **QQ** as a precursor. The product distribution of this kind of precursor is highly sensitive to variations in reaction conditions, including the polarity of the reaction medium, as well as the molar ratios of substrates and reagents (Yoon et al. 2000; Defant et al. 2006; Kadela et al. 2016). Regarding the nucleophilic reactivity of unsymmetrical heterocyclic quinones such as chlorinated **QQ**, it is important to note that the two chlorine atoms present are not equivalent, and substitution by amines occurs predominantly at the chlorine atom positioned at C-6 and/or C-7, depending on the reaction medium and reagents employed (Kadela-Tomanek et al. 2017; Santoso et al. 2019). Earlier studies have demonstrated that amination at the C-6 position significantly influences the biological activity of QQ derivatives. In the literature, it has been reported that the presence of Lewis acids, such as $NiCl_2 0.6\ H_2O$ or $CeCl_3 0.7\ H_2O$, as catalysts promotes preferential substitution at C-6. This selectivity arises from the reduction of electron density at C-6 through chelation of the Lewis acid, specifically Ce(III), between the nitrogen atom of the pyridine ring and the oxygen atom at the C-8 position (Yoon et al. 2000; Lee et al. 2004). Additionally, the use of polar solvents such as water or ethanol has been shown to further favour substitution at the C-6 position (Yoon et al. 2000). As shown in Scheme 1, the synthesis of the library of aminated QQs (**AQQ1-13**) was initiated by the addition of $CeCl_3 0.7\ H_2O$ as a Lewis acid to promote the substitution at the C-6 position, followed by amination, which led to the final products (**AQQ1-13**). The reaction yields varied depending on the nature of the aromatic amine substrates, ranging from low to moderate yields. This variation may be attributed to the electronic and steric properties of the substituents, which can influence both the reactivity and stability of the intermediates formed during the reaction.

The chemical structure of the aminated QQs (**AQQ1-13**) was verified by physicochemical and spectral analyses by means of Fourier-transform infrared spectroscopy (FTIR), nuclear magnetic resonance (NMR), and mass spectrometry (MS). In the FTIR spectra, the 3200–3300 cm^{-1} band revealed the formation of N-H. The carbonyl group (>C=O) of quinone moiety showed characteristic bands at around 1600–1700 cm^{-1}. Moreover, the CH stretch of the aromatic group showed at about 3100 cm^{-1}. All the protons of NH of the sulfonamide moiety gave a downfield broad singlet at around 11.00–12.00 ppm while all the protons of NH of the



Scheme 1 Synthesis of the QQ and generation of **AQQ1-13** by its regioselective amination

aromatic amine appeared at around 9.50 ppm. The electronegativity of nitrogen atom at the N-1 position in quinolinequinone resulted in larger chemical values at around 2.66 ppm for the protons of methyl group attached to the carbon atom at the C-2 position in quinolinequinone in comparison with the protons of the acetyl group in **AQQ1** (1.93 ppm). The signal for protons of the methoxy group were observed at around 3.80 ppm. The chemical shifts of protons of the methyl group(s) in heterocyclic moieties appeared at around 2.90, 2.30, and 1.60 ppm. From the ^{13}C NMR spectra, the signals of the 180.0 and 175.0 ppm could be seen for the carbonyl of quinone moiety. The signals of the aliphatic carbons were observed at around 6–26 ppm while the methyl carbons attached to the oxygen atom (methoxy group) were detected at around 55 ppm.

Antimicrobial activity

Determination of minimum inhibitory concentrations (MIC)

To evaluate the effect of the aromatic amine moiety with a sulfonamide group combined with heterocyclic or acyl substituents, the in vitro antibacterial and antifungal activities of AQQ1-13 were assessed against clinically important four strains of Gram-negative bacteria (*Pseudomonas aeruginosa* ATCC 27853, *Escherichia coli* ATCC 25922, *Klebsiella pneumoniae* ATCC 4352, and *Proteus mirabilis* ATCC 14153), three strains of Gram-positive bacteria (*Enterococcus faecalis* ATCC 29212, *Staphylococcus epidermidis* ATCC 12228, and *Staphylococcus aureus* ATCC 29213) and three strains of fungi (*Candida albicans* ATCC 10231, *Candida parapsilosis* ATCC 22019, and *Candida tropicalis* ATCC 750) with the positive control of clinical drugs (ceftazidime, cefuroxime-Na, cefuroxime, amikacin, clotrimazole, and amphotericin B) as illustrated in Table 1. The minimum inhibitory concentration (MIC, μg/mL) is defined as the lowest concentration of **AQQ1-13** that the lowest concentration that inhibits visible microbial growth. The synthesized aminated AQQs exhibited no or very low antibacterial activity against Gram-negative bacteria, with MIC values generally greater than 2500 μg/mL. **AQQ11** showed weak activity against *E. coli* with an MIC of 312.50 μg/mL, while four compounds (**AQQ2**, **AQQ5**, **AQQ6**, and **AQQ9**) showed limited activity against *K. pneumoniae* with MIC values of 625 μg/mL. Four AQQs (**AQQ3**, **AQQ5**, **AQQ6**, and **AQQ11**) displayed poor activity against *P. mirabilis*

Table 1 The MIC values of the aminated QQs (**AQQ1-13**) for antimicrobial activity.[a]

ID	Microorganisms									
	Bacteria							Fungi (MIC, μg/mL)		
	Gram-negative Bacteria (MIC, μg/mL)				Gram-positive Bacteria (MIC, μg/mL)			Fungi (MIC, μg/mL)		
	P. aeruginosa	*E. coli*	*K. pneumoniae*	*P. mirabilis*	*E. faecalis*	*S. epidermidis*	*S. aureus*	*C. albicans*	*C. parapsilosis*	*C. tropicalis*
AQQ1	-	-	-	-	-	-	-	78.12	-	-
AQQ2	-	-	625	-	-	-	-	312.50	625	-
AQQ3	-	-	-	625	312.50	-	-	-	312.50	-
AQQ4	-	-	-	-	-	-	-	312.50	625	-
AQQ5	-	625	625	625	156.25	625	625	**19.53**	**39.06**	**19.53**
AQQ6	-	-	625	625	625	-	625	156.25	78.12	156.25
AQQ7	-	-	-	-	-	-	-	156.25	625	-
AQQ8	-	-	-	-	-	-	-	312.50	-	-
AQQ9	-	-	625	-	-	-	-	312.50	625	-
AQQ10	-	-	-	-	-	625	-	78.12	-	-
AQQ11	-	312.50	-	625	312.50	312.50	625	39.06	-	-
AQQ12	-	-	-	-	-	-	-	-	-	-
AQQ13	-	-	-	-	-	-	-	156.25	156.25	156.25
ceftazidime	2.44	n.d.	n.d.	n.d.	n.d.	n.d.	n.d.	n.d.	n.d.	n.d.
cefuroxime-Na	n.d.	4.88	4.88	2.44	n.d.	n.d.	1.22	n.d.	n.d.	n.d.
cefuroxime	n.d.	n.d.	n.d.	n.d.	n.d.	9.76	n.d.	n.d.	n.d.	n.d.
amikacin	n.d.	n.d.	n.d.	n.d.	128	n.d.	n.d.	n.d.	n.d.	n.d.
clotrimazole	n.d.	n.d.	n.d.	n.d.	n.d.	n.d.	n.d.	4.88	n.d.	n.d.
amphotericin B	n.d.	n.d.	n.d.	n.d.	n.d.	n.d.	n.d.	n.d.	0.5	1.0

[a] "-" means > 2500 μg/mL activity.

"n.d." means not determined.

with MICs of 625 µg/mL. The results in Table 1 reveal that the obtained compounds showed relatively higher activity compared to Gram-negative bacteria against Gram-positive bacteria. Results against *E. faecalis* revealed that two compounds (***AQQ3*** *and* ***AQQ11***) showed inhibitory activity with MIC values of 312.50 µg/mL, whereas **AQQ5** showed higher activity with MIC value of 156.25 µg/mL. On the other side, most of the AQQs were almost inactive against *S. epidermidis*, except that three AQQs (**AQQ5**, **AQQ10**, and **AQQ11**) showing weak activity with MIC values of 625 and 312.50 µg/mL, respectively. Taken into consideration against *S. aureus*, *most of the AQQs remained inactive except for* **AQQ5**, **AQQ6**, and **AQQ11** (MIC = 625 µg/mL). Overall, the antifungal activity of the compounds was more pronounced compared to their antibacterial effects. Moreover, **AQQ1**, **AQQ10**, and **AQQ11**, with MIC values ranging from 39.06 to 78.12 µg/mL, had moderate antifungal activity against *C. albicans*, although lower than that of the reference antifungal agent clotrimazole (MIC = 4.88 µg/mL). **AQQ5** demonstrated the highest activity among the tested compounds with MIC value of 19.53 µg/mL against *C. albicans*, although still lower than the standard reference clotrimazole. Three AQQs (**AQQ3**, **AQQ6**, and **AQQ13**) demonstrated activity against *C. parapsilosis* (MIC values between 78.12 and 312.50 µg/mL), while **AQQ6** and **AQQ13** exhibited activity against *C. tropicalis*. Among the tested compounds, **AQQ5** was the most active compound against three fungi and may serve as a basis for further optimization.

For this reason, we evaluated the antifungal activity against 25 different clinical *Candida* spp. samples isolated from blood specimens. The tested compounds exhibited high MIC values (> 250 µg/mL) against clinical *Candida* spp. isolates, in contrast to the results obtained with ATCC strains. These findings suggest that the activity of the tested molecule may be affected by antifungal resistance mechanisms present in clinical isolates. At this point, these results highlight the importance of evaluating compounds not only against standard ATCC strains but also against clinical isolates to better assess their potential therapeutic relevance.

Determination of time-kill curve kinetic study

TKC studies were conducted on the *C. albicans* ATCC 10,231 strain. The TKC demonstrated that neither the tested molecule nor the antifungal agent exhibited fungicidal activity against the investigated strain at both 1x and 4x MIC within 24 h. On the other hand, when **AQQ5** was combined with fluconazole at both 1x and 4x MIC, the additive effect was observed (with a 1 $\log_{10}$ reduction). No antagonism was detected in any combination.

Fig. 3 (**A**) ClustalX multiple alignment showing conservation data for farnesyl pyrophosphate synthase from *Homo sapiens*, *Candida albicans*, *Candida parapsilosis*, and *Candida tropicalis*. Ligand binding residues are highlighted in yellow, blue arrow indicates metal binding residues, red arrow indicates isoprenyl binding residues and magenta arrow indicates dimethyl allyl pyrophosphate binding residues; (**B**) Reactions catalysed by farnesyl pyrophosphate synthase enzyme; (**C**) Nitrogen containing bisphosphonate (NBP) inhibitors of farnesyl pyrophosphate synthase in clinical use; (**D**) Non-NBP containing inhibitors of farnesyl pyrophosphase synthase in literature; (**E**) Magnesium and Risendronic acid (RIS) modelled Candida albicans farnesyl pyrophosphate synthase. Magnesium ions represented as magenta balls, metal binding residues represented as cyan sticks coloured by heteroatoms, RIS represented as gray sticks coloured with heteroatom and metal interactions represented as magenta dashed lines. IPPI: Isopentenyl pyrophosphate isomerase, FPPS: Farnesyl pyrophosphate synthase

Even if this combination did not show synergistic activity, its additive compatibility with fluconazole, an antifungal agent frequently used in the treatment of *Candida* spp. infections in the clinic, reveals the potential usage for adding to the combination for lowering toxicity and preventing antifungal resistance as a combination agent of the molecule in the future.

Molecular docking study

We selected compound **AQQ5** for molecular docking studies using human farnesyl pyrophosphate synthase (PDB ID: 5CG5) as the structural reference, because it showed promising antifungal activity against the fungal species used in the study. We attempted to identify the probable target for this compound through SwissTargetPrediction server (http://www.swisstargetprediction.ch/). A total of 100 targ et proteins in human was predicted by the server. Subsequently, STRING server (https://string-db.org/) identified one orthologous protein in *C. albicans*, Farnesyl pyrophosphate synthase (FPPS, EC: 2.5.1.10). Sequence identity of ~45% have been observed between *Homo sapiens* and *C. albicans*/*C. parapsilosis*/*C. tropicalis*, while ~ 84–90% have been observed between the three *Candida* species (Fig. 3A). All the metal binding residues and substrate binding residues in Site 1 (isoprenyl binding site) and Site 2 (dimethyl allyl pyrophosphate binding site) are highly conserved in human and the three *Candida* species (Fig. 3A; Table 2) with similar substrate binding pocket (active site) geometry.

FPPS is a metalloenzyme having 3 magnesium ions in the active site catalysing the biosynthesis of farnesyl pyrophosphate (FPP) from isopentenyl pyrophosphate (IPP) and geranyl pyrophosphate (GPP) (Fig. 3B). FPP is essential for the biosynthesis of ergosterol, a major component of fungal cell membrane. Accordingly, a compound interfering the catalytic reaction of FPPS will in turn adversely affect the cell membrane formation during replication and growth phase. Nitrogen-containing bisphosphonate (NBP, Fig. 3C) inhibitors of

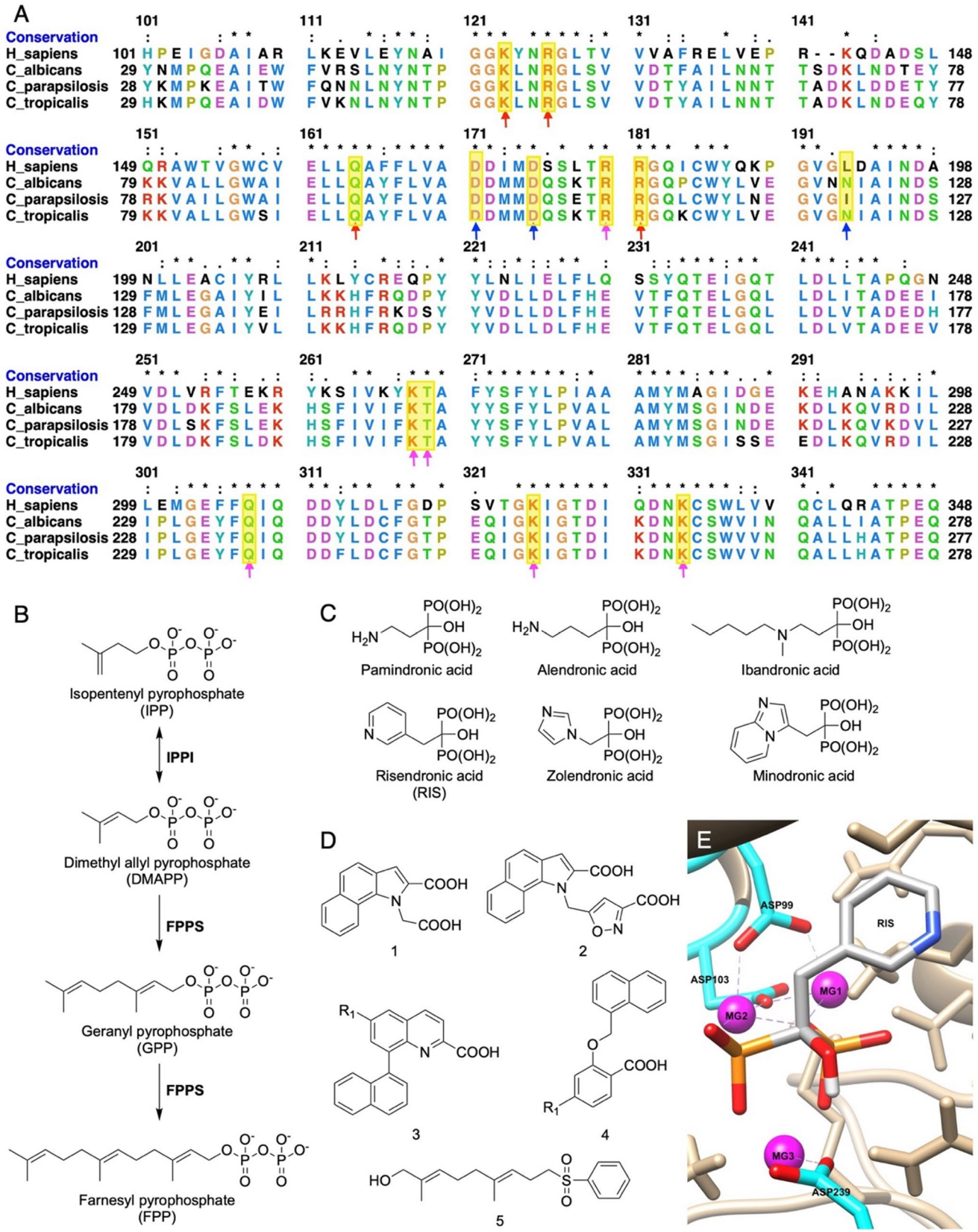

A
Conservation
H_sapiens
C_albicans
C_parapsilosis
C_tropicalis
B
Isopentenyl pyrophosphate (IPP)
IPPI
Dimethyl allyl pyrophosphate (DMAPP)
FPPS
Geranyl pyrophosphate (GPP)
FPPS
Farnesyl pyrophosphate (FPP)
C
Pamindronic acid
Alendronic acid
Ibandronic acid
Risendronic acid (RIS)
Zolendronic acid
Minodronic acid
D
1
2
3
4
5
E
ASP99
RIS
ASP103
MG1
MG2
MG3
ASP239

Table 2 Conservation of active site pocket residues

Region	H. sapiens	C. albicans	C. parapsilosis	C. tropicalis
Metal binding residues (Acidic in nature)	ASP169	ASP99	ASP98	ASP99
	ASP173	ASP103	ASP102	ASP103
	LEU192	ASN122	ILE121	ASN122
Isoprenyl binding site (Site 1-Basic in nature)	LYS123	LYS51	LYS50	LYS51
	ARG126	ARG54	ARG53	ARG54
	GLN162	GLN92	GLN91	GLN92
	ARG179	ARG109	ARG108	ARG109
Dimethyl allyl pyrophosphate binding site (Site 2-Basic in nature)	ARG178	ARG108	ARG107	ARG108
	LYS 266	LYS196	LYS195	LYS196
	THR267	THR197	THR196	THR197
	GLN 306	GLN236	GLN235	GLN236
	LYS 323	LYS253	LYS252	LYS253
	LYS332	LYS262	LYS261	LYS262

Colour coding: Red for acidic amino acids, Blue for basic amino acids, Cyan for neutral amino acids, and Black for hydrophobic amino acids.

human FPPS (hFPPS) are well known for their antiosteoporotic (El- Sayed et al. 2024), anticancer (Khedr et al. 2023), and diabetic cardiomyopathy (Liu et al. 2023). Non-NBP inhibitors (Fig. 3D) invariably contain a carboxylic acid group as bioisosteric replacement for phosphate(Park et al. 2020). They were also evaluated for their parasiticidal and insecticidal activity as there is a high sequence identity between their FPPS with hFPPS (Park et al. 2020). We found a previous docking study and a whole-cell activity-based reports against *Candida albicans* FPPS (caFPPS) (Prokopenko et al. 2014; Metelytsia et al. 2019). A farnesol mimic with sulphate (bioisostere of phosphate, compound **5**, Fig. 3D) has also been reported for its caFPPS inhibitory activity as a reason for its antifungal activity (Fairlamb et al. 2003).

X-ray crystallographic structure of hFPPS co-crystallized with NBPs clearly shown the interaction of bisphosphonate group with the 3 magnesium ions in the catalytic site (Yokoyama et al. 2015). The non-bisphosphonate containing inhibitors of FPPS invariably contain carboxylic acid or sulphonic acid functional groups as an (bio)isostere for phosphonate. Compound **AQQ5** has two metal chelating pharmacophoric features, quinolinequinone and acidic sulphanilamide linked with heterocyclic ring (thiadiazole) at the C-6 position of quinolinequinone. Based on the basic nature of dimethylallylpyrophosphate binding site (Site 2), it is expected that acidic sulphonamide group to interact with magnesium ions, while quinoline quinone ring system to occupy the polar isoprenyl binding site (Site 1).

As the X-ray crystallographic 3D-structure of the fungal protein was not available in protein data bank (https://www.rcsb.org/), we build the one through AlphaFold on google colab (Jumper et al. 2021; Kim et al. 2025) for the purpose of molecular docking study. Sequence for the protein caFPPS was obtained from Uniprot KB (ID: A0A8H6BTG9). The modelled fungal protein was overlapped on to human farnesyl pyrophosphate synthase (PDB ID: 5CG5) (Yokoyama et al. 2015) to get the coordinate of three magnesium ions (and RIS, co-crystallized ligand in 5CG5), as shown in Fig. 3E. Modelled protein was then used for molecular docking study.

Compound **AQQ5** is well accommodated in the active site of caFPPS (Fig. 4). Quinone oxygen at C-8 position established three H-bonding interactions with the sidechain functional groups of ARG54 and GLN92, both the residues belong to Site 1. While quinone oxygen at C-4 position established H-bonding interaction with side chain amino functional group of LYS253, a Site 2 residue. This has facilitated hydrophobic interaction and π-cation interaction with LYS253 and ARG108 residues, respectively for nitrogen containing six-membered ring of quinolinequinone. These interactions positioned the C-7 chloro functional group to engage with sidechain phenolic-OH of TYR200 through halogen bonding interaction. Further, two more H-bonding interactions were observed, one between -NH at C-6 position and side chain of GLN236 and the other one between sulphonamide -NH and side chain of ASP257 were instrumental in orienting the sulphanilamide segment in the space between three Mg^{2+} ions. As expected, this electron rich acidic segment interacts with the Mg^{2+} ions the way the nitrogen containing-bisphosphonates do. Overall, the compound **AQQ5** displays interactions with residues in ligand binding site as well as with catalytic Mg^{2+} ion in the active site. As metal binding residues and ligand binding residues are completely conserved in *C. albicans* and *C. tropicalis*, **AQQ5** shows antifungal activity at strikingly similar concentrations. A single amino acid variation at position 122 (121 in *C. parapsilosis*), ASN122(polar)→ILE121(non-polar), lead to the approximately two-fold higher concentration (MIC) against *C. parapsilosis*. Given the close alignment of observations with experimental findings, Farnesyl pyrophosphate synthase is likely to be the putative target of **AQQ5**.

In silico ADMET studies

Physico-chemical properties and drug-likeness were predicted through SwissADME server (http://www.swissadme.ch/) for compound **AQQ5**. It was found to comply with Lipinski Ro5 with low aqueous solubility and low GI absorption (intestinal permeation) leading to Abbott bioavailability score of 0.55. Salt formation may improve aqueous solubility which in turn may positively influence the intestinal permeation. It is also

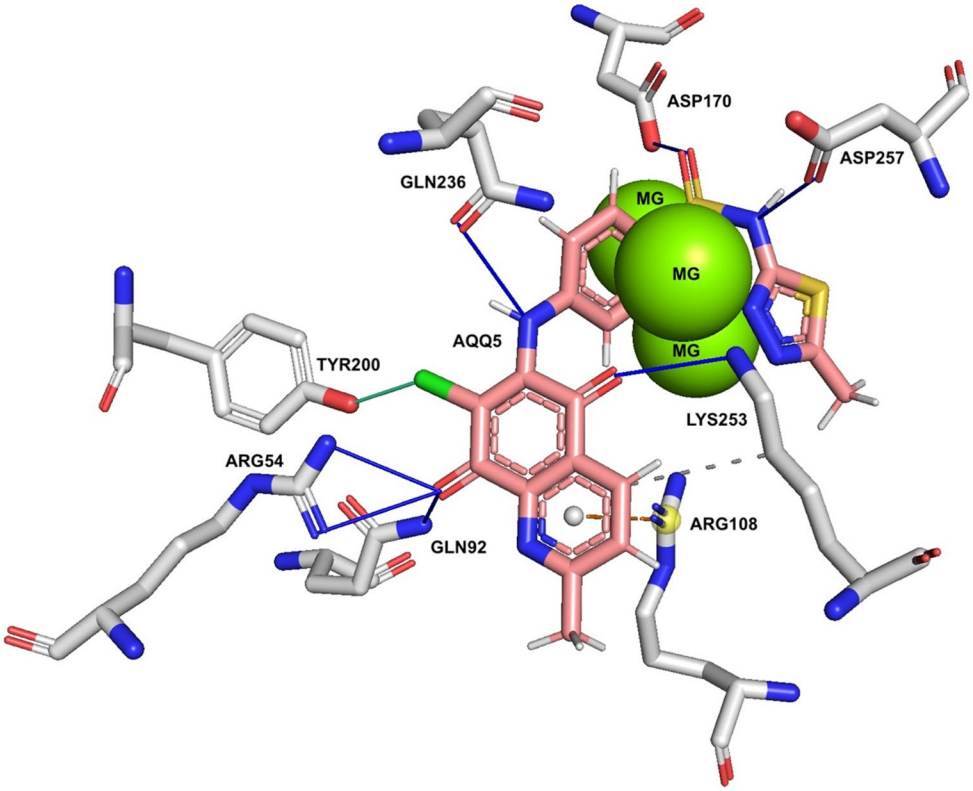


Fig. 4 Interaction of **AQQ5** with *Candida albicans* Farnesyl diphosphate synthase (UniprotKB ID: A0A8H6BTG9). Amino acid residues are represented as tube form coloured by atom type with carbon in light gray; compound **AQQ5** represented in tube form coloured by atom type with carbon in peach orange; magnesium ions are represented as green spheres; hydrogen bonding interactions are shown as blue lines, hydrophobic interaction as gray dotted lines, halogen interaction as green line and π-cation interaction as orange dotted line (between aromatic centre represented as grey ball and cationic centre as yellow ball)

predicted to have no blood brain barrier (BBB) permeation and may not be useful in treating fungal meningitis, encephalitis and brain abscess. Similarly, they are predicted to inhibit CYP2C19, 2C9 and 3A4 and may possibly influence the pk-profile of drugs metabolized by these enzymes. **AQQ5** is not a substrate to *p*-glycoprotein (efflux-pump), means they may withstand development of resistance through efflux-pump. Another major concern is that they tend to show two PAINS alert due to the presence of halo-enone and quinone portion. While in silico ADMET studies are not so encouraging, the selective antifungal activity of the compound warrants further LEAD optimization program through active analogue approach to improve both potency as well as pharmacokinetic profile of the compound.

Conclusions

In the current study, we have focused on the synthesis of a series of aminated QQs (**AQQ1-13**) and assessed them for their antibacterial and antifungal activities. Based on our previous findings, commercially available aromatic amines were selected according to the substituents attached to the benzene ring. Within this study, aromatic amines containing a sulfonamide group with heterocyclic substituent (isoxazole, thiadiazole, pyridine, pyrimidine, pyrazine, and pyridazine) or acyl group (acetyl or benzamide) with different substituents were selected. Compound **AQQ5** (MIC = 19.53 µg/mL) showed the highest antifungal activity against *C. albicans*. Moreover, **AQQ5** also exhibited the highest activity against two other fungi (*C. parapsilosis* and *C. tropicalis*). However, this activity was observed only against ATCC strains. Considering the increasing prevalence of antifungal resistance, results obtained using only ATCC strains may not fully reflect activity against clinical isolates. Therefore, evaluating compounds against clinical isolates, in addition to standard strains, is important for a more comprehensive assessment of their antimicrobial potential. Therefore, based on the data we obtained, we would like to emphasize that this situation may cause an underestimation. However, the molecular docking studies suggested that **AQQ5** exhibited favourable interactions with its putative target farnesyl pyrophosphate synthase (caFPPS). Further, direct interaction studies (biochemical or biophysical) may position this compound in a distinct class of Non-NBP caFPPS inhibitors effective against fungal infections.

Experimental

Chemicals and apparatus

Chemicals and solvents were commercially available and used as received with a minimum purity of 95% used

without further purification unless otherwise stated. Thin-layer chromatography (TLC) was performed on silica gel TLC plates with a fluorescence indicator at 254 nm using aluminium-based DC-plates (Silica gel 60 F_{254}, Merck). Column chromatography was performed using silica gel 60 (63–200 µm particle-sized) with an appropriate solvent system as eluent. TLC plates were visualized using UV light (254–365 nm). Melting points (mp) were determined on a Büchi B-540 melting point apparatus and were uncorrected. Mass spectra were obtained on a BRUKER Microflex LT with a MALDI (Matrix Assisted Laser Desorption Ionization)-TOF technique by adding a matrix. High-Resolution Mass Spectrometry (HRMS) analyses was recorded on a Waters SYNAPT G1 MS (Waters, USA). The infrared (IR) spectra were recorded on an FTIR spectrometer, using the single reflection diamond ATR module. All the NMR spectra were recorded on a Bruker Avance III HD spectrometer with deuterated solvent $CDCl_3$ and tetramethyl silane (TMS) used as an internal standard. Chemical shifts were reported in parts per million (ppm, δ), and coupling constants (J) were given in hertz (Hz). The purity of the synthesized compounds was determined by high-performance liquid chromatography (HPLC) analysis using a Shimadzu DGU-20A5 system equipped with a 25 cm Chiralpak AD-H column. The mobile phase was acetonitrile. The flow rate was 1.0 mL/min, and detection was carried out at 254 nm. All compounds were found to have a purity of ≥95%.

Procedure for the synthesis of the quinolinequinone (QQ)

6,7-Dichloro-2-methyl-5,8-quinolinequinone (**QQ**) was prepared according to the literature from 2-methyl-8-quinolinol and sodium chlorate in concentrated HCl in 12% yield (Shaikh et al. 1986). Mp 179–180 ºC (Lit. 180–181 ºC (Shaikh et al. 1986). ^{1}H NMR (500 MHz, *CDCl$_3$*) δ (ppm): 8.31 (d, J=8.30 Hz, 1H, $CH_{aromatic}$), 7.53 (d, J=8.30 Hz, 1H, $CH_{aromatic}$), 2.73 (s, 3 H, CH_3). ^{13}C NMR (125 MHz, *CDCl$_3$*) δ (ppm): 174.6, 173.5 (2>C=O), 165.1, 145.3, 142.9, 141.8, 134.6, 127.2, 125.2 ($C_{aromatic}$ and C_q), 24.3 (CH_3). MS (+ESI) *m/z* (%): 242 (100, $[M+H]^+$), 240 (11, $[M-H]^+$). Anal. Calcd. for $C_{10}H_5Cl_2NO_2$ (240.97).

General procedure for the synthesis of aminated quinolinequinones (AQQ1-13)

A suspension of the **QQ** (0.150 g, 0.620 mmol) and $CeCl_3.7H_2O$ (0.253 g, 0.682 mmol, 1.1 equiv) in ethanol was stirred at room temperature for 45 min. Then, to a solution of **QQ** and $CeCl_3.7H_2O$, the corresponding aromatic amines (0.682 mmol, 1.1 equiv) in ethanol were successively added, and the reaction mixture was stirred for 16 h until complete consumption of **QQ**. After evaporation of the solvent, the residue was dissolved with $CHCl_3$ (50 mL), and the solution was washed sequentially with water (3 × 30 mL). The organic layer was dried over $CaCl_2$, filtered, and concentrated under reduced pressure. The reaction crude was purified on a silica gel column chromatography using the eluent system to give the corresponding AQQs.

N-(4-[(7-chloro-2-methyl-5,8-dioxo-5,8-dihydroquinolin-6-yl)amino]phenylsulfonyl)acetamide (AQQ1)

By subjecting the mixture (**QQ** and $CeCl_3.7H_2O$) and sulfacetamide (0.097 g, 0.454 mmol) to the general procedure for the synthesis of the **AQQ1**, the title compound (**AQQ1**) was purified by column chromatography on silica gel using hexane/ethyl acetate (5:2, v/v) as eluent to afford the title compound as a red solid. Yield: 11%, mp 228–229 °C. FTIR (ATR) υ (cm^{-1}): 3315 (NH), 3033 ($CH_{aromatic}$), 2837, 2793, 2685 ($CH_{aliphatic}$), 1718, 1682 (2>C=O), 1655, 1588, 1569, 1531, 1476, 1405, 1370, 1344, 1304, 1293, 1259, 1224, 1200, 1182, 1158 (SO_2), 1143, 1115, 1091, 1032. ^{1}H NMR (500 MHz, *DMSO-d$_6$*) δ (ppm): 11.99 (br s, 1H, $NHSO_2$), 9.61 (s, 1H, NH), 8.30 (d, J=8.0 Hz, 1H, $CH_{aromatic}$), 7.80 (d, J=8.6 Hz, 2 H, $CH_{aromatic}$), 7.69 (d, J=8.0 Hz, 1H, $CH_{aromatic}$), 7.25 (d, J=8.5 Hz, 2 H, $CH_{aromatic}$), 2.67 (s, 3 H, CH_3), 1.93 (s, 3 H, CH_3). ^{13}C NMR (125 MHz, *DMSO-d$_6$*) δ (ppm): 180.07, 176.24 (2>C=O), 169.21, 164.73, 147.49, 144.67, 142.43, 135.24, 133.29, 128.36, 127.57, 126.25, 122.85, 122.06, 121.19 ($C_{aromatic}$ and C_q), 25.09, 23.73 (CH_3). MS (MALDI-TOF, DIT matrix) *m/z*: 421 $[M+2H]^+$; Anal. Calcd. for $C_{18}H_{14}ClN_3O_5S$ (419.03).

N-(4-[(7-chloro-2-methyl-5,8-dioxo-5,8-dihydroquinolin-6-yl)amino]phenylsulfonyl)benzamide (AQQ2)

By subjecting the mixture (**QQ** and $CeCl_3.7H_2O$) and sulfabenzamide (0.188 g, 0.682 mmol) to the general procedure for the synthesis of the **AQQ2**, the title compound (**AQQ2**) was purified by column chromatography on silica gel using hexane/ethyl acetate (5:2, v/v) as eluent to afford the title compound as a red solid. Yield: 32%, mp 170.9–174.9 °C. FTIR (ATR) υ (cm^{-1}): 3300 (NH), 3070 ($CH_{aromatic}$), 2867 ($CH_{aliphatic}$), 1679, 1573 (2>C=O), 1514, 1453, 1435, 1346, 1295, 1256, 1162 (SO_2), 1086, 1064, 1027. ^{1}H NMR (500 MHz, *DMSO-d$_6$*) δ (ppm): 12.42 (br s, 1H, $NHSO_2$), 9.63 (s, 1H, NH), 8.29 (d, J=8.0 Hz, 1H, $CH_{aromatic}$), 7.91–7.87 (m, 3 H, $CH_{aromatic}$), 7.63 (t, J=8.2 Hz, 2 H, $CH_{aromatic}$), 7.50 (t, J=7.8 Hz, 3 H, $CH_{aromatic}$), 7.28 (d, J=8.3 Hz, 2 H, $CH_{aromatic}$), 2.67 (s, 3 H, CH_3). ^{13}C NMR (125 MHz, *DMSO-d$_6$*) δ (ppm): 180.06, 176.22 (2>C=O), 165.96, 164.73, 154.18, 147.48, 144.67, 142.42, 135.23, 133.65, 130.54, 129.06, 128.87, 128.60, 127.55, 126.23, 124.18, 122.09,

112.71 ($C_{aromatic}$ and C_q), 25.09 (CH_3). MS (MALDI-TOF, DHB matrix) *m/z*: 482 $[M+H]^+$; Anal. Calcd. for $C_{23}H_{16}ClN_3O_5S$ (481.05).

4-[(7-chloro-2-methyl-5,8-dioxo-5,8-dihydroquinolin-6-yl) amino]-N-(5-methylisoxazol-3-yl)benzenesulfonamide (AQQ3)

By subjecting the mixture (**QQ** and $CeCl_3.7H_2O$) and sulfamethoxazole (0.173 g, 0.682 mmol) to the general procedure for the synthesis of the **AQQ3**, the title compound (**AQQ3**) was purified by column chromatography on silica gel using hexane/ethyl acetate (5:2, v/v) as eluent to afford the title compound as a red solid. Yield: 35%, mp 235.9–237.4 °C. FTIR (ATR) υ (cm^{-1}): 3178 (NH), 3006 ($CH_{aromatic}$), 2989, 2900, 2848 ($CH_{aliphatic}$), 1675, 1649 (2>C=O), 1623, 1607, 1574, 1511, 1468, 1402, 1319, 1302, 1272, 1226, 1164 (SO_2), 1143, 1091, 1036. ^{1}H NMR (500 MHz, *DMSO-d_6*) δ (ppm): 11.32 (br s, 1H, $NHSO_2$), 9.57 (br s, 1H, NH), 8.29 (d, *J*=7.7 Hz, 1H, $CH_{aromatic}$), 7.75–7.68 (s, 3 H, $CH_{aromatic}$), 7.23 (d, *J*=8.3 Hz, 2 H, $CH_{aromatic}$), 6.15 (s, 1H, $CH_{aromatic}$), 2.67 (s, 3 H, CH_3), 2.30 (s, 3 H, CH_3). ^{13}C NMR (125 MHz, *DMSO-d_6*) δ (ppm): 180.03, 176.17 (2>C=O), 170.68, 164.70, 158.09, 147.47, 144.30, 142.39, 135.19, 133.52, 127.49, 126.19, 122.45, 120.87, 95.89 ($C_{aromatic}$ and C_q), 25.08, 12.53 (CH_3). MS (MALDI-TOF, DIT matrix) *m/z*: 460 $[M+2\ H]^+$; Anal. Calcd. for $C_{20}H_{15}ClN_4O_5S$ (458.05).

4-[(7-chloro-2-methyl-5,8-dioxo-5,8-dihydroquinolin-6-yl) amino]-N-(3,4-dimethylisoxazol-5-yl)benzenesulfonamide (AQQ4)

By subjecting the mixture (**QQ** and $CeCl_3.7H_2O$) and sulfisoxazole (0.182 g, 0.682 mmol) to the general procedure for the synthesis of the **AQQ4**, the title compound (**AQQ4**) was purified by column chromatography on silica gel using hexane/ethyl acetate (5:2, v/v) as eluent to afford the title compound as a purple solid. Yield: 54%, mp 228–229 °C. FTIR (ATR) υ (cm^{-1}): 3219, 3156 (NH), 3093, 3022 ($CH_{aromatic}$), 2785 ($CH_{aliphatic}$), 1707, 1679, 1656 (2>C=O), 1644, 1588, 1569, 1520, 1492, 1405, 1368, 1341, 1322, 1297, 1261, 1228, 1204, 1189, 1162 (SO_2), 1143, 1117, 1104, 1091, 1032, 1008. ^{1}H NMR (500 MHz, *DMSO-d_6*) δ (ppm): 10.94 (br s, 1H, $NHSO_2$), 9.62 (s, 1H, NH), 8.29 (d, *J*=8.0 Hz, 1H, $CH_{aromatic}$), 7.73–7.59 (m, 3 H, $CH_{aromatic}$), 7.25 (d, *J*=8.6 Hz, 2 H, $CH_{aromatic}$), 2.67 (s, 3 H, CH_3), 2.09 (s, 3 H, CH_3), 1.63 (s, 3 H, CH_3). ^{13}C NMR (125 MHz, *DMSO-d_6*) δ (ppm): 180.11, 176.24 (2>C=O), 164.76, 161.88, 156.09, 147.49, 144.28, 142.44, 135.21, 134.10, 127.57, 127.38, 126.16, 122.71, 120.50, 105.61 ($C_{aromatic}$ and C_q), 25.08, 10.80, 6.29 (CH_3). MS (MALDI-TOF, DIT matrix) *m/z*: 472 $[M]^+$; Anal. Calcd. for $C_{21}H_{17}ClN_4O_5S$ (472.06).

4-[(7-chloro-2-methyl-5,8-dioxo-5,8-dihydroquinolin-6-yl)amino]-N-(5-methyl-1,3,4-thiadiazol-2-yl) benzenesulfonamide (AQQ5)

By subjecting the mixture (**QQ** and $CeCl_3.7H_2O$) and sulfamethizole (0.184 g, 0.682 mmol) to the general procedure for the synthesis of the **AQQ5**, the title compound (**AQQ5**) was purified by column chromatography on silica gel using hexane/ethyl acetate (5:2, v/v) as eluent to afford the title compound as a red solid. Yield: 35%, mp=270 °C (dec.). FTIR (ATR) υ (cm^{-1}): 3281, 3172 (NH), 2893 ($CH_{aliphatic}$), 1672, 1662 (2>C=O), 1607, 1573, 1535, 1509, 1437, 1407, 1297, 1221, 1139 (SO_2), 1085, 1038. ^{1}H NMR (500 MHz, *DMSO-d_6*) δ (ppm): 9.54 (s, 1H, NH), 8.28 (d, *J*=7.9 Hz, 1H, $CH_{aromatic}$), 7.76–7.54 (m, 4 H, $CH_{aromatic}$), 7.21 (d, *J*=8.5 Hz, 2 H, $CH_{aromatic}$), 2.66 (s, 3 H, CH_3), 2.47 (s, 3 H, CH_3). ^{13}C NMR (125 MHz, *DMSO-d_6*) δ (ppm): 180.07, 176.12 (2>C=O), 168.15, 164.70, 154.93, 147.48, 143.35, 142.48, 136.53, 135.18, 127.46, 126.36, 126.11, 122.72, 119.84 ($C_{aromatic}$ and C_q), 25.06, 16.51 (CH_3). MS (MALDI-TOF, NOM) *m/z*: 477 $[M+2\ H]^+$; Anal. Calcd. for $C_{19}H_{14}ClN_5O_4S_2$ (475.02).

4-[(7-chloro-2-methyl-5,8-dioxo-5,8-dihydroquinolin-6-yl) amino]-N-(pyridin-2-yl)benzenesulfonamide (AQQ6)

By subjecting the mixture (**QQ** and $CeCl_3.7H_2O$) and sulfapyridine (0.170 g, 0.682 mmol) to the general procedure for the synthesis of the **AQQ6**, the title compound (**AQQ6**) was purified by column chromatography on silica gel using hexane/ethyl acetate (5:2, v/v) as eluent to afford the title compound as a red solid. Yield: 24%, mp 162.5–164.2 °C. FTIR (ATR) υ (cm^{-1}): 3290 (NH), 3104, 3056, 3030 ($CH_{aromatic}$), 2985, 2815, 2756 ($CH_{aliphatic}$), 1677, 1662 (2>C=O), 1632, 1608, 1574, 1523, 1461, 1387, 1355, 1307, 1286, 1271, 1243, 1223, 1174, 1145, 1136 (SO_2), 1110, 1084, 1042, 1001. ^{1}H NMR (500 MHz, *DMSO-d_6*) δ (ppm): 9.51 (br s, 1H, NH), 8.38–8.21 (m, 2 H, $CH_{aromatic}$), 8.03 (s, 1H, $CH_{aromatic}$), 7.83–7.63 (m, 4 H, $CH_{aromatic}$), 7.22–7.10 (m, 3 H, $CH_{aromatic}$), 6.88 (s, 1H, $CH_{aromatic}$), 2.66 (s, 3 H, CH_3). ^{13}C NMR (125 MHz, *DMSO-d_6*) δ (ppm): 180.08, 176.12 (2>C=O), 164.70, 147.51, 143.07, 142.53, 135.17, 127.46, 127.25, 126.10, 122.66, 119.72 ($C_{aromatic}$ and C_q), 25.08 (CH_3). MS (MALDI-TOF, DHB matrix) *m/z*: 457 $[M+3\ H]^+$; Anal. Calcd. for $C_{21}H_{15}ClN_4O_4S$ (454.05); HRMS(-ESI) m/z calcd for $C_{21}H_{14}ClN_4O_4S$ $[M-H]^+$: 453.0424; found: 453.0370.

4-[(7-chloro-2-methyl-5,8-dioxo-5,8-dihydroquinolin-6-yl) amino]-N-(pyrimidin-2-yl)benzenesulfonamide (AQQ7)

By subjecting the mixture (**QQ** and $CeCl_3.7H_2O$) and sulfadiazine (0.114 g, 0.454 mmol) to the general procedure for the synthesis of the **AQQ7**, the title compound (**AQQ7**) was

purified by column chromatography on silica gel using hexane/ethyl acetate (5:2, v/v) as eluent to afford the title compound as a red solid. Yield: 14%, mp 228–229 °C. ^{1}H NMR (500 MHz, *DMSO-d_6*) δ (ppm): 11.70 (br s, 1H, $NHSO_2$), 9.55 (s, 1H, NH), 8.51 (d, J=4.8 Hz, 2 H, $CH_{aromatic}$), 8.28 (d, J=8.0 Hz, 1H, $CH_{aromatic}$), 7.89 (d, J=8.3 Hz, 2 H, $CH_{aromatic}$), 7.68 (d, J=8.0 Hz, 1H, $CH_{aromatic}$), 7.22 (d, J=8.4 Hz, 2 H, $CH_{aromatic}$), 7.06 (t, J=4.8 Hz, 1H, $CH_{aromatic}$), 2.66 (s, 3 H, CH_3). ^{13}C NMR (125 MHz, *DMSO-d_6*) δ (ppm): 180.09, 176.20 (2>C=O), 164.73, 158.82, 157.42, 147.50, 143.87, 142.49, 135.21, 128.34, 127.52, 126.16, 122.27, 120.30 ($C_{aromatic}$ and C_q), 25.09 (CH_3). MS (MALDI-TOF, DIT matrix) *m/z*: 457 $[M+2\,H]^+$; Anal. Calcd. for $C_{20}H_{14}ClN_5O_4S$ (455.05).

4-[(7-chloro-2-methyl-5,8-dioxo-5,8-dihydroquinolin-6-yl)amino]-N-(4,6-dimethylpyrimidin-2-yl) benzenesulfonamide (AQQ8)

By subjecting the mixture (**QQ** and $CeCl_3.7H_2O$) and sulfamethazine (0.190 g, 0.682 mmol) to the general procedure for the synthesis of the **AQQ8**, the title compound (**AQQ8**) was purified by column chromatography on silica gel using hexane/ethyl acetate (5:2, v/v) as eluent to afford the title compound as a red solid. Yield: 46%, mp=200 °C (dec.). FTIR (ATR) υ (cm^{-1}): 3304 (NH), 3087, 3011 ($CH_{aromatic}$), 2800 ($CH_{aliphatic}$), 1684, 1631 (2>C=O), 1599, 1560, 1551, 1546, 1488, 1437, 1409, 1379, 1346, 1307, 1265, 1232, 1208, 1186, 1147 (SO_2), 1119, 1090, 1036. ^{1}H NMR (500 MHz, *DMSO-d_6*) δ (ppm): 11.42 (br s, 1H, $NHSO_2$), 9.57 (d, 1H, $CH_{aromatic}$), 8.27 (d, J=7.4 Hz, 1H, $CH_{aromatic}$), 7.89 (d, J=8.3 Hz, 2 H, $CH_{aromatic}$), 7.70–7.66 (m, 1H, $CH_{aromatic}$), 7.21 (d, J=8.0 Hz, 2 H, $CH_{aromatic}$), 6.76 (s, 1H, NH), 2.65 (s, 3 H, CH_3), 2.25 (s, 6 H, CH_3). ^{13}C NMR (125 MHz, *DMSO-d_6*) δ (ppm): 180.13, 178.78 (2>C=O), 177.10, 176.15, 164.74, 163.66, 156.67, 147.52, 146.68, 143.73, 143.42, 142.52, 135.18, 134.79, 128.74, 128.35, 127.33, 126.10, 122.13 ($C_{aromatic}$ and C_q), 25.08, 24.86, 23.32 (CH_3). MS (MALDI-TOF, DHB matrix) *m/z*: 483 $[M]^+$; Anal. Calcd. for $C_{22}H_{18}ClN_5O_4S$ (483.08).

4-[(7-chloro-2-methyl-5,8-dioxo-5,8-dihydroquinolin-6-yl) amino]-N-(5-methoxypyrimidin-2-yl)benzenesulfonamide (AQQ9)

By subjecting the mixture (**QQ** and $CeCl_3.7H_2O$) and sulfameter (0.127 g, 0.454 mmol) to the general procedure for the synthesis of the **AQQ9**, the title compound (**AQQ9**) was purified by column chromatography on silica gel using hexane/ethyl acetate (5:2, v/v) as eluent to afford the title compound as a red solid. Yield: 10%, mp 228–229 °C. FTIR (ATR) υ (cm^{-1}): 3322, 3289 (NH), 3093, 3033 ($CH_{aromatic}$), 2919, 2848, 2807, 2726 ($CH_{aliphatic}$), 1661, 1607 (2>C=O), 1574, 1514, 1484, 1426, 1403, 1337, 1317, 1304, 1277, 1256, 1215, 1176, 1162 (SO_2), 1141, 1088, 1036, 1014. ^{1}H NMR (500 MHz, *DMSO-d_6*) δ (ppm): 11.39 (br s, 1H, $NHSO_2$), 9.55 (s, 1H, NH), 8.33–8.27 (m, 3 H, $CH_{aromatic}$), 7.86 (d, J=8.6 Hz, 2 H, $CH_{aromatic}$), 7.68 (d, J=8.0 Hz, 1H, $CH_{aromatic}$), 7.21 (d, J=8.6 Hz, 2 H, $CH_{aromatic}$), 3.80 (s, 3 H, OCH_3), 2.67 (s, 3 H, CH_3). ^{13}C NMR (125 MHz, *DMSO-d_6*) δ (ppm): 180.11, 176.20 (2>C=O), 164.73, 151.46, 150.13, 147.52, 145.11, 143.78, 142.49, 135.21, 134.76, 128.18, 127.52, 126.17, 122.26, 120.33 ($C_{aromatic}$ and C_q), 56.75 (OCH_3), 25.09 (CH_3). MS (MALDI-TOF, DIT matrix) *m/z*: 485 $[M]^+$; Anal. Calcd. for $C_{21}H_{16}ClN_5O_5S$ (485.06).

4-[(7-chloro-2-methyl-5,8-dioxo-5,8-dihydroquinolin-6-yl) amino]-N-(6-methoxypyrimidin-4-yl)benzenesulfonamide (AQQ10)

By subjecting the mixture (**QQ** and $CeCl_3.7H_2O$) and sulfamonomethoxine (0.191 g, 0.682 mmol) to the general procedure for the synthesis of the **AQQ10**, the title compound (**AQQ10**) was purified by column chromatography on silica gel using hexane/ethyl acetate (5:2, v/v) as eluent to afford the title compound as a red solid. Yield: 26%, mp 232.9–234.2 °C. FTIR (ATR) υ (cm^{-1}): 3211 (NH), 3081 ($CH_{aromatic}$), 2959, 2925, 2856 ($CH_{aliphatic}$), 1675, 1623 (2>C=O), 1570, 1511, 1480, 1389, 1350, 1289, 1219, 1200, 1142 (SO_2), 1087, 1036. ^{1}H NMR (500 MHz, *DMSO-d_6*) δ (ppm): 9.56 (s, 1H, NH), 8.41 (s, 1H, $CH_{aromatic}$), 8.26 (d, J=7.9 Hz, 1H, $CH_{aromatic}$), 7.82 (d, J=8.5 Hz, 2 H, $CH_{aromatic}$), 7.66 (d, J=7.9 Hz, 1H, $CH_{aromatic}$), 7.23 (d, J=8.4 Hz, 2 H, $CH_{aromatic}$), 6.35 (s, 1H, $CH_{aromatic}$), 3.84 (s, 3 H, OCH_3), 2.65 (s, 3 H, CH_3). ^{13}C NMR (125 MHz, *DMSO-d_6*) δ (ppm): 180.00, 176.12 (2>C=O), 170.37, 164.72, 158.93, 147.43, 143.96, 142.42, 135.17, 127.66, 127.50, 126.11, 122.52, 120.46, 91.35 ($C_{aromatic}$ and C_q), 54.65 (OCH_3), 25.06 (CH_3). MS (MALDI-TOF, NOM) *m/z*: 487 $[M+2\,H]^+$; Anal. Calcd. for $C_{21}H_{16}ClN_5O_5S$ (485.06).

4-[(7-chloro-2-methyl-5,8-dioxo-5,8-dihydroquinolin-6-yl)amino]-N-(2,6-dimethoxypyrimidin-4-yl) benzenesulfonamide (AQQ11)

By subjecting the mixture (**QQ** and $CeCl_3.7H_2O$) and sulfadimethoxine (0.141 g, 0.454 mmol) to the general procedure for the synthesis of the **AQQ11**, the title compound (**AQQ11**) was purified by column chromatography on silica gel using hexane/ethyl acetate (5:2, v/v) as eluent to afford the title compound as a red solid. Yield: 6%, mp 228–229 °C. FTIR (ATR) υ (cm^{-1}): 3259 (NH), 3100 ($CH_{aromatic}$), 2924, 2852 ($CH_{aliphatic}$), 1677, 1570 (2>C=O), 1507, 1474, 1381, 1355, 1320, 1296, 1204, 1147 (SO_2), 1102, 1091,

1064, 1025. ^{1}H NMR (500 MHz, *DMSO-d_6*) δ (ppm): 11.50 (br s, 1H, $NHSO_2$), 9.58 (s, 1H, NH), 8.28 (d, J=8.0 Hz, 1H, $CH_{aromatic}$), 7.83 (d, J=8.5 Hz, 2 H, $CH_{aromatic}$), 7.68 (d, J=8.0 Hz, 1H, $CH_{aromatic}$), 7.24 (d, J=8.6 Hz, 2 H, $CH_{aromatic}$), 5.95 (s, 1H, $CH_{aromatic}$), 3.80 (s, 3 H, OCH_3), 3.76 (s, 3 H, OCH_3), 2.67 (s, 3 H, CH_3). ^{13}C NMR (125 MHz, *DMSO-d_6*) δ (ppm): 180.09, 176.20 (2>C=O), 172.14, 164.73, 160.49, 147.50, 144.20, 142.46, 135.21, 127.98, 127.54, 126.20, 122.42, 120.66, 85.08 ($C_{aromatic}$ and C_q), 55.00, 54.28 (OCH_3), 25.09 (CH_3). MS (MALDI-TOF, DHB matrix) *m/z*: 516 $[M+H]^+$; Anal. Calcd. for $C_{22}H_{18}ClN_5O_6S$ (515.07).

4-[(7-chloro-2-methyl-5,8-dioxo-5,8-dihydroquinolin-6-yl) amino]-N-(6-methoxypyridazin-3-yl)benzenesulfonamide (AQQ12)

By subjecting the mixture (**QQ** and $CeCl_3.7H_2O$) and sulfamethoxypyridazine (0.191 g, 0.682 mmol) to the general procedure for the synthesis of the **AQQ12**, the title compound (**AQQ12**) was purified by column chromatography on silica gel using hexane/ethyl acetate (5:2, v/v) as eluent to afford the title compound as a red solid. Yield: 64%, mp 89.3–91.2 °C. FTIR (ATR) υ (cm^{-1}): 3247 (NH), 3074 ($CH_{aromatic}$), 2952 ($CH_{aliphatic}$), 1675 (2>C=O), 1570, 1524, 1468, 1406, 1294, 1223, 1136 (SO_2), 1084, 1003. ^{1}H NMR (500 MHz, *DMSO-d_6*) δ (ppm): 9.53 (s, 1H, NH), 8.28 (d, J=7.7 Hz, 1H, $CH_{aromatic}$), 7.74 (d, J=6.9 Hz, 4 H, $CH_{aromatic}$), 7.67 (d, J=7.7 Hz, 1H, $CH_{aromatic}$), 7.38 (d, J=8.9 Hz, 1H, $CH_{aromatic}$), 7.20 (d, J=6.8 Hz, 2 H, $CH_{aromatic}$), 3.84 (s, 3 H, OCH_3), 2.66 (s, 3 H, CH_3). ^{13}C NMR (125 MHz, *DMSO-d_6*) δ (ppm): 180.08, 176.10 (2>C=O), 172.45, 164.71, 147.49, 142.96, 142.53, 135.16, 127.45, 126.77, 126.08, 122.75, 119.56 ($C_{aromatic}$ and C_q), 54.95 (OCH_3), 25.05 (CH_3). MS (MALDI-TOF, NOM) *m/z*: 487 $[M+2\ H]^+$; Anal. Calcd. for $C_{21}H_{16}ClN_5O_5S$ (485.06).

4-[(7-chloro-2-methyl-5,8-dioxo-5,8-dihydroquinolin-6-yl) amino]-N-(3-methoxypyrazin-2-yl)benzenesulfonamide (AQQ13)

By subjecting the mixture (**QQ** and $CeCl_3.7H_2O$) and sulfalene (0.191 g, 0.682 mmol) to the general procedure for the synthesis of the **AQQ13**, the title compound (**AQQ13**) was purified by column chromatography on silica gel using hexane/ethyl acetate (5:2, v/v) as eluent to afford the title compound as a red solid. Yield: 18%, mp 215.3–217.2 °C. FTIR (ATR) υ (cm^{-1}): 3296, 3206 (NH), 3078 ($CH_{aromatic}$), 2959, 2919 ($CH_{aliphatic}$), 1673, 1655 (2>C=O), 1571, 1557, 1509, 1470, 1439, 1383, 1346, 1319, 1302, 1224, 1202, 1165, 1154 (SO_2), 1088, 1036, 1003. ^{1}H NMR (500 MHz, *DMSO-d_6*) δ (ppm): 10.79 (br s, 1H, $NHSO_2$), 9.55 (s, 1H, NH), 8.28 (d, J=8.0 Hz, 1H, $CH_{aromatic}$), 7.89 (d, J=8.7 Hz, 2 H, $CH_{aromatic}$), 7.81–7.70 (m, 2 H, $CH_{aromatic}$), 7.68 (d, J=8.3 Hz, 1H, $CH_{aromatic}$), 7.22 (d, J=8.6 Hz, 2 H, $CH_{aromatic}$) 3.91 (s, 3 H, OCH_3), 2.66 (s, 3 H, CH_3). ^{13}C NMR (125 MHz, *DMSO-d_6*) δ (ppm): 180.14, 176.06 (2>C=O), 164.70, 150.28, 147.96, 143.86, 142.72, 142.52, 138.42, 135.17, 134.95, 133.62, 128.38, 128.21, 127.53, 126.12, 122.24, 120.69 ($C_{aromatic}$ and C_q), 54.19 (OCH_3), 25.07 (CH_3). MS (MALDI-TOF, NOM) *m/z*: 487 $[M+2\ H]^+$; Anal. Calcd. for $C_{21}H_{16}ClN_5O_5S$ (485.06).

Biological studies

Determination of biological activity

The minimum inhibitory concentrations (MICs) of the substances were evaluated using the broth microdilution technique approved by the Clinical and Laboratory Standards Institute (CLSI) (1997; 2020). Three Gram-negative bacteria (*Pseudomonas aeruginosa* ATCC 27853, *Klebsiella pneumoniae* ATCC 4352, and *Proteus mirabilis* ATCC 14153), four Gram-positive bacteria (*Staphylococcus aureus* ATCC 29213, *Staphylococcus epidermidis* ATCC 12228, and *Enterococcus faecalis* ATCC 29212) and three fungi (*Candida albicans* ATCC 10231, *Candida parapsilosis* ATCC 22019, and *Candida tropicalis* ATCC 750) were cultured following CLSI protocols. The stock solutions of the analysed substances were prepared in DMSO. Serial two-fold dilutions ranging from 1250 to 0.06 µg/mL were prepared in Mueller Hinton Broth. The inoculum was prepared using a 4–6 h broth culture of each bacteria and 24 h culture of yeast strains adjusted to a turbidity equivalent of a 0.5 McFarland standard, diluted in broth media to give a final concentration of 5×10^5 CFU/mL for bacteria and 0.5×10^3 to 2.5×10^3 CFU/mL for yeast in the test tray. The trays were covered and placed in plastic bags to prevent evaporation. The trays containing Mueller-Hinton broth were incubated at 35 °C for 18–20 h while the trays containing RPMI-1640 medium were incubated at 35 °C for 46–50 h. The MIC was defined as the lowest concentration of tested extracts that demonstrated complete inhibition of visible growth. Experiments were performed in triplicate.

Based on the antibacterial activity data, we sought to ascertain the in vitro efficacy of **AQQ5** against clinically isolated Candida spp. strains using the broth microdilution method as outlined by CLSI guidelines. For this experiment, 25 unique, Candida spp. isolated from blood specimens were procured from the Clinical Microbiology Laboratories of Group Florence Nightingale Hospitals in Turkey. Isolates were identified with Vitek 2 (BioMerieux, Craponne, France) and verified with API 20 C AUX (BioMerieux, France) (Aydın et al. 2024).

Determination of time-kill curves

The fungicidal and synergistic activity of selected molecule, which was chosen based on its MIC value, **AQQ5** alone or in combination with conventional antifungal, fluconazole, was assessed using the time-kill curve (TKC) method at one and four times the MIC against *C. albicans* ATCC 10,231 strain (Mataraci-Kara et al. 2020, 2022a). Molecule-free controls were included for the tested strain. The test tubes containing RPMI with and without (growth control) molecule in a final volume of 10 mL were incubated in a 37 °C calibrated shaking water bath, and viable counts were determined at 0, 2, 4, 6, and 24 h intervals after inoculation by subculturing 0.1 mL serial dilutions onto SDA plates. All tests were performed in triplicate. The lower limit of detection for the time-kill assay was 1 $\log_{10}$ CFU/mL.

The fungicidal activity was defined as a ≥ 3 $\log_{10}$ CFU/mL reduction from the initial inoculum. The impact of combining the data was analysed in relation to its more potent component. Synergy and antagonism were described as a 2 $\log_{10}$ reduction or increase in the viable count of the combination after 24 h relative to the more active of the two drugs when used alone, respectively.

Molecular docking and ADMET analysis

AlphaFold modelled *Candida albicans* Farnesyl pyrophosphate synthase (caFPPS) was initially prepared for molecular docking simulation using Dock Prep utility in Chimera (Pettersen et al. 2004; Yang et al. 2012) and subsequently processed using MGLTools-1.5.7 (Morris et al. 2009). Structure of **AQQ5** was prepared through SwissParm server (http://swissparam.ch/) and converted for docking with MGLTools-1.5.7. Docking calculations were carried out using autodock4, and affinity maps were generated with autogrid4. For docking the grid box of dimension $40 \times 40 \times 40$ was centred around the reference ligand RIS in the active site. For docking of **AQQ5**, 300 genetic algorithm runs were applied and, the remaining parameters were left as the default AutoDock4 setting. The obtained binding poses were grouped based on the AutoDock4 clustering method. The highest scoring conformer from the largest cluster was selected to make the protein-ligand complex which was further analysed through PLIP server (Salentin et al. 2015; Adasme et al. 2021).

Supplementary Information The online version contains supplementary material available at https://doi.org/10.1007/s12223-026-01489-z.

Author contributions Formal analysis and investigation, H. Y., M.Y., N. B., B. Ö., E. M.-K., M. H., (A) B., (B) Ö.-Ç., V. J., and A. F. T.; Supervision, (A) F. T.; Conceptualization, E. M.-K., (B) Ö.-Ç., V. J., and (A) F. T.; Methodology, H. Y., M.Y., N. B., (B) Ö., E. M.-K., M. H., (A) B., (B) Ö.-Ç., V. J., and A. F. T.; Writing - original draft preparation, E. M.-K., V. J., and (A) F. T.; Writing - review and editing, H. Y., M.Y., N. B., (B) Ö., E. M.-K., M. H., (A) B., (B) Ö.-Ç., V. J., and A. F. T. All the authors have reviewed and approved the final version of the manuscript.

Funding Open access funding provided by the Scientific and Technological Research Council of Türkiye (TÜBİTAK). This work was financially supported by the Scientific Research Projects Coordination Unit of Istanbul University (Project numbers: FYO-2021-38298) for supplying the equipment and materials.

Data availability No datasets were generated or analysed during the current study.

Declarations

Competing interests The authors declare no competing interests.

Clinical trial number Not applicable.

Open Access This article is licensed under a Creative Commons Attribution 4.0 International License, which permits use, sharing, adaptation, distribution and reproduction in any medium or format, as long as you give appropriate credit to the original author(s) and the source, provide a link to the Creative Commons licence, and indicate if changes were made. The images or other third party material in this article are included in the article's Creative Commons licence, unless indicated otherwise in a credit line to the material. If material is not included in the article's Creative Commons licence and your intended use is not permitted by statutory regulation or exceeds the permitted use, you will need to obtain permission directly from the copyright holder. To view a copy of this licence, visit http://creativecommons.org/licenses/by/4.0/.

References

Adasme MF, Linnemann KL, Bolz SN, Kaiser F, Salentin S, Haupt VJ, Schroeder M (2021) PLIP 2021: expanding the scope of the protein-ligand interaction profiler to DNA and RNA. Nucleic Acids Res 49:W530–W534. https://doi.org/10.1093/nar/gkab294

Alberts B, Johnson A, Lewis J, Raff M, Roberts K, Walter P (2002) Plant development. Molecular biology of the cell, 4th edn. pp 1471–1520. Garland Science

Alexander BD, Johnson MD, Pfeiffer CD et al (2013) Increasing Echinocandin Resistance in Candida glabrata: Clinical Failure Correlates With Presence of FKS Mutations and Elevated Minimum Inhibitory Concentrations. Clin Infect Dis 56:1724–1732. https://doi.org/10.1093/cid/cit136

Alfadhli A, Mack A, Harper L et al (2016) Analysis of quinolinequinone reactivity, cytotoxicity, and anti-HIV-1 properties. Bioorg Med Chem 24:5618–5625. https://doi.org/10.1016/j.bmc.2016.09.028

Arendrup M (2014) Update on antifungal resistance in Aspergillus and Candida. Clin Microbiol Infect 20:42–48. https://doi.org/10.1111/1469-0691.12513

Aydin M, Hacioglu M, Inan N (2024) Comparison of the inhibition of Candida spp biofilm formation by quorum-sensing molecules, farnesol and tyrosol with amphotericin B. Istanbul J Pharm 54:189–194. https://doi.org/10.26650/IstanbulJPharm.2024.1417841

Chan-Zapata I, Borges-Argáez R, Ayora-Talavera G (2023) Quinones as promising compounds against respiratory viruses: a review. Molecules 28:1981. https://doi.org/10.3390/molecules28041981

Chen C, Pawley SB, Cote JM et al (2024) Identification of triazolyl KAT6 inhibitors via a templated fragment approach. Bioorg Med Chem Lett 113:129948. https://doi.org/10.1016/j.bmcl.2024.129948

Clinical and Laboratory Standards Institute (1997) Reference method for broth dilution antifungal susceptibility testing of yeasts; approved standard–second edition. Wayne, PA, USA

Clinical and Laboratory Standards Institute (2020) Performance standards for antimicrobial susceptibility testing. 30th ed. CLSI supplement M100 (ISBN 978-1-68440-066-9 [Print]; ISBN 978-1-68440-067-6 [Electronic], Clin Lab Stand Inst, 950 West Valley Road, Suite 2500, Wayne, Pennsylvania 19087, USA.

Cochran GM, Ewald PW, Cochran KD (2000) Infectious causation of disease: an evolutionary perspective. Perspect Biol Med 43:406–448. https://doi.org/10.1353/pbm.2000.0016

Dahlem Junior MA, Nguema Edzang RW, Catto AL, Raimundo JM (2022) Quinones as an efficient molecular scaffold in the antibacterial, antifungal or antitumoral arsenal. Int J Mol Sci 23:14108. https://doi.org/10.3390/ijms232214108

de Carvalho AS, da Rocha DR, Ferreira VF (2021) Strategies for the Synthesis of Mono- and Bis-Thionaphthoquinones. Curr Org Synth 18:535–546. https://doi.org/10.2174/1570179418666210224124603

Defant A, Mancini I (2019) Design, Synthesis and Cancer Cell Growth Inhibition Evaluation of New Aminoquinone Hybrid Molecules. Molecules 24:2224. https://doi.org/10.3390/molecules24122224

Defant A, Guella G, Mancini I (2006) Regioselectivity in the multicomponent synthesis of indolizinoquinoline-5,12-dione derivatives. Eur J Org Chem 2006:4201–4210. https://doi.org/10.1002/ejoc.200600317

Devi M, Kumar P, Singh R et al (2022) A comprehensive review on synthesis, biological profile and photophysical studies of heterocyclic compounds derived from 2,3-diamino-1,4-naphthoquinone. J Mol Struct 1269:133786. https://doi.org/10.1016/j.molstruc.2022.133786

Egu SA, Ibezim A, Onoabedje EA, Okoro UC (2017) Biological and In silico Evaluation of Quinolinedione and Naphthoquinone Derivatives as Potent Antibacterial Agents. ChemistrySelect 2:9222–9226. https://doi.org/10.1002/slct.201700692

El-Sayed NF, El-Hussieny M, Mansour ST et al (2024) Farnesyl pyrophosphate synthase inhibitors with antiosteoporosis efficacy in ovariectomized rats: A mixed binding approach beyond bisphosphonates. Eur J Med Chem 276:116679. https://doi.org/10.1016/j.ejmech.2024.116679

Elgemeie GH, Azzam RA, Elsayed RE (2019) Sulfa drug analogs: new classes of N-sulfonyl aminated azines and their biological and preclinical importance in medicinal chemistry (2000–2018). Med Chem Res 28:1099–1131. https://doi.org/10.1007/s00044-019-02378-6

Elsayad KA, Elmasry GF, Mahmoud ST, Awadallah FM (2024) Sulfonamides as anticancer agents: A brief review on sulfonamide derivatives as inhibitors of various proteins overexpressed in cancer. Bioorg Chem 147:107409. https://doi.org/10.1016/j.bioorg.2024.107409

Fairlamb IJ, Dickinson JM, O'Connor R et al (2003) Synthesis and antimicrobial evaluation of farnesyl diphosphate mimetics. Bioorg Chem 31:80–97. https://doi.org/10.1016/S0045-2068(03)00025-7

Hu HY, Zhu Y, Wang L, Xu JH (2005) A direct one-pot synthesis of naphtho[2,3-b]furan-4,9-dione derivatives via C,O-Dialkylation of β-Dicarbonyl compounds by 2,3-Dichloro-1,4-naphthoquinones. Synthesis 2005:1605–1610. https://doi.org/10.1055/s-2005-865305

Ibacache JA, Valderrama JA et al (2016) Antiproliferative Activity of New 6-Bromine Derivatives of 7-Anilino-1-Arylisoquinolinequinones. J Chil Chem Soc 61:3191–3194. https://doi.org/10.4067/S0717-97072016000400008

Ibacache JA, Faundes J, Montoya M et al (2018) Preparation of Novel Homodimers Derived from Cytotoxic Isoquinolinequinones. A Twin Drug Approach. Molecules 23:439. https://doi.org/10.3390/molecules23020439

Jedrzejas MJ (2001) Pneumococcal Virulence Factors: Structure and Function. Microbiol Mol Biol Rev 65:187–207. https://doi.org/10.1128/mmbr.65.2.187-207.2001

Jumper J, Evans R, Pritzel A et al (2021) Highly accurate protein structure prediction with AlphaFold. Nature 596:583–589. https://doi.org/10.1038/s41586-021-03819-2

Kadela M, Jastrzebska M et al (2016) Synthesis, Structure and Cytotoxic Activity of Mono- and Dialkoxy Derivatives of 5,8-Quinolinedione. Molecules 21:156. https://doi.org/10.3390/molecules21020156

Kadela-Tomanek M, Jastrzebska M et al (2017) Alkynyloxy derivatives of 5,8-quinolinedione: Synthesis, in vitro cytotoxicity studies and computational molecular modeling with NAD(P)H:Quinone oxidoreductase 1. Eur J Med Chem 126:969–982. https://doi.org/10.1016/j.ejmech.2016.12.031

Keinan S, Paquette WD et al (2008) Computational design, synthesis and biological evaluation of para-quinone-based inhibitors for redox regulation of the dual-specificity phosphatase Cdc25B. Org Biomol Chem 6:3256–3263. https://doi.org/10.1039/B806712K

Khedr MA, Al-Wabli RI et al (2023) Design, Synthesis, Molecular Docking, Dynamics and in vitro Evaluation of Novel 2-substituted-1-hydroxyethane-1,1-bis(phosphonic acid) Derivatives as Human Farnesyl Pyrophosphate Synthase Inhibitors with Expected Anticancer Activity. Curr Pharm Des 29:48–59. https://doi.org/10.2174/1381612829666221202114947

Kim G, Lee S et al (2025) Easy and accurate protein structure prediction using ColabFold. Nat Protoc 20:620–642. https://doi.org/10.1038/s41596-024-01060-5

Kruschel RD, Buzid A et al (2020) Isoquinolinequinone N-oxides as anticancer agents effective against drug resistant cell lines. Org Biomol Chem 18:557–568. https://doi.org/10.1039/C9OB02441G

Kruschel RD, Barbosa MAG et al (2024) Discovery of Potent Isoquinolinequinone N-Oxides to Overcome Cancer Multidrug Resistance. J Med Chem 67:13909–13924. https://doi.org/10.1021/acs.jmedchem.4c00705

Kuang Y, Sechi M et al (2018) Design and Synthesis of Novel Reactive Oxygen Species Inducers for the Treatment of Pancreatic Ductal Adenocarcinoma. J Med Chem 61:1576–1594. https://doi.org/10.1021/acs.jmedchem.7b01463

Lawrence HR, Kazi A et al (2010) Synthesis and biological evaluation of naphthoquinone analogs as a novel class of proteasome inhibitors. Bioorg Med Chem 18:5576–5592. https://doi.org/10.1016/j.bmc.2010.06.038

Lee HJ, Kim JS et al (2004) Synthesis and cytotoxicity evaluation of 6,11-dihydro-pyridazoand 6,11-dihydro-pyrido[2,3-blphenazine-6,11-diones. Bioorg Med Chem 12:1623–1628. https://doi.org/10.1016/j.bmc.2004.01.029

Liu X, Liu Y et al (2023) Inhibition of farnesyl pyrophosphate synthase alleviates cardiomyopathy in diabetic rat. Cell Cycle 22:666–679. https://doi.org/10.1080/15384101.2022.2139126

Mak TW, Saunders ME (2007) Immunity to pathogens. Immune Response 641–694. https://doi.org/10.1016/B978-012088451-3.50024-7

Martins-Santana L et al (2023) Addressing microbial resistance worldwide: challenges over controlling life-threatening fungal infections. Pathogens 12:293. https://doi.org/10.3390/pathogens12020293

Mataraci-Kara E et al (2020) Evaluation of antifungal and disinfectant-resistant Candida species isolated from hospital wastewater. Arch Microbiol 202:2543–2550. https://doi.org/10.1007/s00203-020-01975-z

Mataraci-Kara E et al (2022a) Discovery and structure-activity relationships of the quinolinequinones: Promising antimicrobial agents and mode of action evaluation. Drug Dev Res 83:628–636. https://doi.org/10.1002/ddr.21893

Mataraci-Kara E et al (2022b) Active Quinolinequinones against Methicillin-Resistant Staphylococcus spp. Chem Biodivers 19:e202100616. https://doi.org/10.1002/cbdv.202100616

Mataraci-Kara E et al (2022c) Exploring the Relationships between Structure and Antimicrobial Potency of Quinolinequinones. Antibiotics 11:1397. https://doi.org/10.3390/antibiotics11101397

Metelytsia L et al (2019) New anti-candida active nitrogen-containing bisphosphonates as inhibitors of farnesyl pyrophosphate synthase Candida albicans. Ukr Biochem J 91:78–89. https://doi.org/10.15407/ubj91.03.078

Mone NS et al (2023) How Structure–Function Relationships of 1,4-Naphthoquinones Combat Antimicrobial Resistance in Multidrug-Resistant (MDR). Pathogens ChemMedChem 18:e202200471. https://doi.org/10.1002/cmdc.202200471

Morris GM et al (2009) AutoDock4 and AutoDockTools4: Automated docking with selective receptor flexibility. J Comput Chem 30:2785–2791. https://doi.org/10.1002/jcc.21256

Naghavi M et al (2024) Global burden of bacterial antimicrobial resistance 1990–2021: a systematic analysis with forecasts to 2050. Lancet 404:1199–1226. https://doi.org/10.1016/S0140-6736(24)01867-1

Navarro-Tovar G et al (2023) The Relevance and Insights on 1,4-Naphthoquinones as Antimicrobial and Antitumoral Molecules: A Systematic Review. Pharmaceuticals 16:496. https://doi.org/10.3390/ph16040496

Park J et al (2020) Phosphonate and Bisphosphonate Inhibitors of Farnesyl Pyrophosphate Synthases: A Structure-Guided Perspective. Front Chem 8:612728. https://doi.org/10.3389/fchem.2020.612728

Pettersen EF et al (2004) UCSF Chimera—A visualization system for exploratory research and analysis. J Comput Chem 25:1605–1612. https://doi.org/10.1002/jcc.20084

Pingaew R et al (2015) Novel 1,4-naphthoquinone-based sulfonamides: Synthesis, QSAR, anticancer and antimalarial studies. Eur J Med Chem 103:446–459. https://doi.org/10.1016/j.ejmech.2015.09.001

Pitout JDD, Laupland KB (2008) Extended-spectrum β-lactamase-producing Enterobacteriaceae: an emerging public-health concern. Lancet Infect Dis 8:159–166. https://doi.org/10.1016/S1473-3099(08)70041-0

Prasad G, Minakshi (2007) Normal microbial flora of human body and host parasite relationship. In Immunology and medical microbiology. National Science Digital Library, Boulder, CO, pp 1–23

Prokopenko V et al (2014) Design and synthesis of new potent inhibitors of farnesyl pyrophosphate synthase. Curr Drug Discov Technol 11:133–144. https://doi.org/10.2174/1570163811310666004 1

Salentin S et al (2015) PLIP: fully automated protein-ligand interaction profiler. Nucleic Acids Res 43:W443–W447. https://doi.org/10.1093/nar/gkv315

Santoso KT et al (2019) The synthesis and evaluation of quinolinequinones as anti-mycobacterial agents. Bioorg Med Chem 27:3532–3545. https://doi.org/10.1016/j.bmc.2019.06.002

Shaikh IA et al (1986) Streptonigrin.1. Structure-Activity-Relationships among Simple Bicyclic Analogs - Rate Dependence of DNA-Degradation on Quinone Reduction Potential. J Med Chem 29:1329–1340. https://doi.org/10.1021/jm00158a002

Shapiro-Ilan DI et al (2005) Definitions of pathogenicity and virulence in invertebrate pathology. J Invertebr Pathol 88:1–7. https://doi.org/10.1016/j.jip.2004.10.003

Sharma S et al (2023) Discovery of a highly potent, selective, orally bioavailable inhibitor of KAT6A/B histone acetyltransferases with efficacy against KAT6A-high ER+ breast cancer. Cell Chem Biol 30:1191–1210e1120. https://doi.org/10.1016/j.chembiol.2023.07.005

Shen DQ et al (2010) Synthesis and antiproliferative activity of indolizinophthalazine-5,12-dione derivatives, DNA topoisomerase IB inhibitors. Eur J Med Chem 45:3938–3942. https://doi.org/10.1016/j.ejmech.2010.05.048

Uysal S et al (2021) Design, synthesis and biological evaluation of novel naphthoquinone-4-aminobenzensulfonamide/carboxamide derivatives as proteasome inhibitors. Eur J Med Chem 209:112890. https://doi.org/10.1016/j.ejmech.2020.112890

Valderrama J et al (1999) Synthesis and in vitro antiprotozoal activity of thiophene ring-containing quinones. Chem Pharm Bull (Tokyo) 47:1221–1226. https://doi.org/10.1248/cpb.47.1221

Valderrama JA et al (2016) Synthesis and Cytotoxic Activity on Human Cancer Cells of Novel Isoquinolinequinone-Amino Acid Derivatives. Molecules 21:1199. https://doi.org/10.3390/molecules21091199

Wellington KW (2015) Understanding cancer and the anticancer activities of naphthoquinones - a review. RSC Adv 5:20309–20338. https://doi.org/10.1039/C4RA13547D

Yang Z et al (2012) UCSF Chimera, MODELLER, and IMP: an integrated modeling system. J Struct Biol 179:269–278. https://doi.org/10.1016/j.jsb.2011.09.006

Yanni AS et al (1991) SYNTHESIS OF SOME NEW SULFONAMIDE DERIVATIVES OF 7-CHLOROQUINOLINE-5,8-DIONE AND PYRIDOCARBAZOLEDIONES. Collect Czech Chem Commun 56:1489–1494. https://doi.org/10.1135/cccc19911489

Yildirim H et al (2022a) Aminated Quinolinequinones as Privileged Scaffolds for Antibacterial Agents: Synthesis, In Vitro Evaluation, and Putative Mode of Action. ACS Omega 7:41915–41928. https://doi.org/10.1021/acsomega.2c03193

Yildirim H et al (2022b) Highly Active Small Aminated Quinolinequinones against Drug-Resistant Staphylococcus aureus and Candida albicans. Molecules 27:2923. https://doi.org/10.3390/molecules27092923

Yokoyama T et al (2015) Protonation State and Hydration of Bisphosphonate Bound to Farnesyl Pyrophosphate Synthase. J Med Chem 58:7549–7556. https://doi.org/10.1021/acs.jmedchem.5b01147

Yoon EY et al (2000) The regioselectivity in the reaction of 6,7-dihaloquinoline-5,8-diones with amine nucleophiles in various solvents. Tetrahedron Lett 41:7475–7480. https://doi.org/10.1016/S0040-4039(00)01278-8

Publisher's Note Springer Nature remains neutral with regard to jurisdictional claims in published maps and institutional affiliations.